Published in *Polymer Degradation and Stability* 168 (2019) 108944

Development of dose-response functions for historic paper degradation using exposure to natural conditions and multivariate regression

Gianluca Pastorelli[a,*,1], Shuo Cao[a,2], Irena Kralj Cigić[b], Costanza Cucci[c], Abdelrazek Elnaggar[d,3], Matija Strlič[a]

[a]UCL Institute for Sustainable Heritage, University College London, 14 Upper Woburn Place, London WC1H 0NN, UK.

[b]Faculty of Chemistry and Chemical Technology, University of Ljubljana, Večna pot 113, 1000 Ljubljana, Slovenia.

[c]Institute of Applied Physics "Nello Carrara" IFAC, Italian National Research Council CNR, Via Madonna del Piano 10, 50019 Sesto Fiorentino (FI), Italy.

[d]Conservation Department, Faculty of Archaeology, Fayoum University, Fayoum, Egypt.

*Corresponding author:

Gianluca Pastorelli

Centre for Art Technological Studies and Conservation, Statens Museum for Kunst, Sølvgade 48-50, 1307 Copenhagen K, Denmark

Email: gianluca.pastorelli@smk.dk

Present addresses:

[1]Centre for Art Technological Studies and Conservation, Statens Museum for Kunst, Sølvgade 48-50, 1307 Copenhagen K, Denmark.

[2]Research Institute of Shenzhen Stock Exchange, 2012 Shennan Blvd., Futian District, Shenzhen, China.

[3]Egypt-Japan University of Science and Technology (E-JUST), Alexandria, Egypt.

Published in *Polymer Degradation and Stability* 168 (2019) 108944

Abstract

Many collections of documents, manuscripts, and works of art on paper are prone to degradation due to a complex interplay of extrinsic and intrinsic factors. The aim of this study was to examine the simultaneous effect of multiple degradation agents on selected non-model types of paper in natural environments, and the relative effect of environmental parameters (heat, humidity, light and pollution) compared to material parameters (pH, fibre composition and presence of additives). An exposure experiment was set up to investigate visual and chemical changes of 12 different types of paper in real time in different environmental conditions over a 1.5-year period at 11 sites across Europe and North Africa, sheltered from UV light and precipitation. Suitable environmental monitoring equipment, such as data loggers and gas samplers, and analytical methods to characterise sample degradation, specifically spectrocolorimetry and capillary viscometry, were used to estimate alterations in visual appearance and degree of cellulose polymerisation, which are the most important properties of paper in the heritage context. Multiple linear regression and principal component regression were used to interpret the large volume of data and calculate a set of dose-response functions. The results of this study not only suggested that most of the considered variables are of significance in relation to changes in colour and in average molecular weight, but also revealed a number of meaningful interactions between these variables. Based on the assessment of the relative contributions of environmental and material-related variables to the natural ageing processes of paper, the dose-response functions proposed in this study enable prioritisation of degradation factors in environmental management of paper-based collections and in historic paper degradation studies; however, further work is required to increase accuracy and understanding of the chemistry of degradation.

Key words

Paper degradation, spectrocolorimetry, capillary viscometry, multiple linear regression, principal component regression, dose-response function.

1 Introduction

1.1 The problem of paper degradation

Paper is the longest-established tangible medium of information, but is also a material inherently susceptible to decay. In the presence of moisture, acids from the environment (derived from air pollution or poor-quality storage materials) or from within the paper (originated from the raw materials, manufacturing process and degradation products) cause chain scission of cellulose. In a typical western archive, library or museum environment, a high percentage of historic documents and works of art made of paper are known to be acidic and therefore prone to degradation via the acid-catalysed hydrolysis process, which, in the long term, may limit their mechanical usability and fitness for display [1]. Beside acid hydrolysis, paper is susceptible to photolytic and oxidative degradation. For this reason, collections of documents, manuscripts, and works of art on paper, such as watercolour paintings, prints, drawings and posters in heritage institutions need to be preserved. The rate and severity of deterioration, as is well known, is the result of internal and external factors, most importantly the chemical properties of paper and the environmental conditions in which the paper is stored [2-5]. Although there are many agents affecting paper degradation during long-term storage and display, they are not all equally damaging or unavoidable. For instance, exposure to light, which can discolour and weaken paper, may be minimised or avoided relatively easily. Pollutants, mainly nitrogen oxides from industrial exhausts, traffic emissions and heating sources, are readily absorbed into paper and may form compounds detrimental to its stability; however, nitrogen dioxide (and to a lesser extent acetic acid) has been shown to affect display lifetimes only in significantly polluted environments, such as those currently found in some rapidly developing economies or in specific microenvironments [6], making the need for chemical air filtration in typical library and archive repositories debatable [7]. Paper composition, acidity probably being the most important parameter, can only be controlled via conservation interventions, e.g. deacidification treatments, that may require financial resources and lead to ethical risks. Moreover, an often-overlooked issue is that some of those degradation factors can have synergistic or antagonistic effects.

1.2 Strategies for collections care

The study and mitigation of degradation processes in paper artefacts is challenging due to the high variability in chemical properties of the material (for example, papers with different content of lignin and different sizing react differently) and to the potential synergistic effects of environmental agents of degradation. Because active treatments may not be sufficient to address the scale of the problem and may cause loss of value, preventive conservation, which aims at reducing the rate of natural ageing by controlling the surrounding environment, becomes the preferred option by conservators of historic paper collections. Knowledge and prioritisation of environmental variables leading to the decay of paper objects are essential to develop suitable preservation strategies for archive, library and museum collections and would allow collection managers to evaluate investments into different environmental control options. Furthermore, the control of environmental effects on paper degradation is relevant not only to the curator and the scientist, but to the user above all.

1.3 Aim of the research

Despite the numerous studies of paper degradation, general dose-response functions taking into account all of the most important environmental agents of deterioration are still absent. Only with such functions, which describe the rate of change of a material property depending on the selected environmental variables, it will be possible to assess and model, for example, which environmental parameters are more important to control than others and which types of paper are more susceptible to particular agents of deterioration. Among the many agents of deterioration, temperature, relative humidity, light, pollution and paper composition have been extensively researched [8] and damage functions focusing only on a selection of the most important environmental variables and materials have been established [9-11]. However, the susceptibility of individual types of historic papers to those agents of deterioration has never been expressed in the form of comprehensive dose-response functions. The scope of this research was therefore to obtain quantitative data on the effects of physical and chemical variables on the degradation of selected types of paper; this data was then processed with advanced statistical methods to develop dose-response functions, based on which environmental management in paper-based collections could be improved to minimise degradation while optimising resource use.

1.4 Approach to the investigation

During long-term storage and display of historic paper documents and works of art at moderate environmental conditions, it is often difficult to assume which environmental agent would have the most decisive influence on the overall behaviour of the material and bring most conservation benefits if controlled. In such instances, investigation of material degradation is experimentally demanding. If no single environmental agent prevails, the number of experimental runs should then be effectively reduced using the principles of statistical experimental design, as was shown in a similar study of degradation of synthetic polymers [12]. In that research, the variables of interest, i.e. temperature, humidity, visible light and typical outdoor-generated primary pollutants, were many, but the number of degradation experiments was reduced significantly, whilst still allowing for effective evaluation of interactions between environmental factors. While the usual method of accelerated degradation in a climate chamber would not allow for all the relevant agents of deterioration to be varied, moderate acceleration of degradation could be achieved by exposing samples to the external environment, with only reasonably exaggerated levels of many environmental variables. In this type of experiments, care needs to be taken that variables that are not relevant indoors are excluded, particularly contact with water and ultraviolet (UV) radiation. Such conditions can be easily achieved in sheltered environments, i.e. well protected from rainfall and direct or reflected sunlight (including UV radiation). However, because environmental variables cannot be controlled, they need to be continuously monitored.

Since the most important properties of paper are those related to its readability and physical usability, specifically visual appearance and mechanical strength, a set of analytical techniques that make it possible to measure changes in these properties were chosen. To determine the alterations in visual properties (i.e. discolouration) of paper, the CIE L*a*b* system, which takes into account the "standard human eye response", was used; as yellowing often characterises paper ageing, b* was used to evaluate changes in colour. Mechanical properties are affected by the acid hydrolysis and oxidative reactions in the cellulose linear homopolymer [2]. The scission of intramolecular bonds results in shorter cellulose chains (as well as in lower paper strength) and leads to a decrease in average molecular weight, which represents the number of monomers in a cellulose polymer (i.e. degree of polymerisation or DP) and can be measured in several ways; in this study, viscometry was used to obtain the viscometric average DP.

2 Materials and methods

2.1 Selection and preparation of samples

Several types of naturally aged papers were chosen, all representative of materials found in historic paper collections and archives. The selected samples (Tab. 1) were well characterised nineteenth to twenty-first century papers containing different pulps (i.e. chemical or bleached pulp, obtained by degrading the lignin into water-soluble molecules which can easily be washed away from the cellulose fibres, and mechanical pulp or groundwood, obtained by physically tearing the cellulose fibres one from another, thus retaining much of the lignin adherent to the fibres) and different sizes or additives, and had been previously studied within the EU FP6 SurveNIR project (SSPI 006594). Additionally, Whatman filter paper (from GE Healthcare Life Sciences, Little Chalfont, UK) made from purified cotton linters cellulose, with no sizing or additives of any kind, was selected as a reference material. Small pieces (some ~ 10 cm × 2 cm and some ~ 4 cm × 4 cm) of the samples listed in Tab. 1 were stapled to a hard polyethylene sheet. This operation was repeated for each of the eight planned exposure period and for each of the 11 exposure sites, producing 88 sample frames in total. The plastic frames (eight for each exposure site) were then vertically hung off a stainless steel wire mesh, protected from three sides with sheets of polyethylene. Three sides were open, allowing for free air circulation (Fig. 1).

Table 1. List of paper samples, with year of production and compositional data, used in the study.

No.	EU FP6 SurveNIR code	Year	pH	Fibre composition (%)			Rosin-based size	Optical brighteners
				Groundwood	Cellulose	Cotton		
1	376	1928	5.8		100		Yes	No
2	395	1915	5.4		30	70	Yes	No
3	567	1906	4.8	5	95		Yes	No
4	688	1894	5.9		80	20	Yes	No
5	775	1942	7.6	10	10	80	Yes	No
6	1002	1935	6.1			100	Yes	No
7	2004	1993	7.7		100		Yes	Yes
8	2042	2001	8		100		No	Yes
9	2141	1964	7.7		100		No	Yes
10	379	1918	4.9	90	10		Yes	No
11	2009	2003	8	30	40	30	No	Yes
12	2031	2002	7.8	15	85		Yes	Yes

Figure 1. Typical sample setups, with individual samples attached to hard polyethylene sheets hanging vertically off a wire mesh and exposed to the environment from three sides.

2.2 Selection of exposure environments

The selection of exposure sites was guided by availability and variability. The list of sites in Tab. 2 shows that the choice was guided by presumed variations in the levels of temperature, relative humidity, light intensity and pollution. Additional details about the exposure sites are discussed elsewhere [12]. The outdoor exposure sites were always very well protected by overhangs or other structures, so that there was no direct or reflected sunlight with the associated UV radiation, which had to be avoided as it is normally not present in archives and other paper collection environments (the absence of UV radiation was verified by preliminary radiometric tests). Each exposure experiment lasted from 6 months to up to 1.5 years.

Table 2. List of exposure sites and their presumed environmental characteristics: '−1' - low; '0' - medium; '1' - high level of heat, humidity, light or pollution.

Reference	Location	Description	Heat	Humidity	Light	Pollution
BB	Bilbao, ES	Suburban, external	0	0	1	1
CA	Cairo, EG	Suburban, internal	1	−1	0	1
FI	Florence, IT	Urban, external	1	1	1	1
LJ1	Ljubljana, SI	Suburban, external	−1	1	−1	−1
LJ2	Ljubljana, SI	Suburban, external	1	1	1	−1
LJ3	Ljubljana, SI	Suburban, internal	1	0	−1	0
LO1	London, UK	Suburban, external	0	1	0	−1
LO2	London, UK	Reference	1	−1	−1	−1
LO3	London, UK	Urban, external	0	1	0	1
MT	Zurrieq, MT	Rural, external	1	1	1	1
RO	Rome, IT	Urban, external	1	0	1	1

2.3 Environmental monitoring

Physical environmental variables, i.e. temperature (T), relative humidity (RH) and visible light illuminance (E_v), were monitored in 30-min intervals with Onset (Cape Cod, MA) HOBO U12 data loggers for the duration of the experiments. The loggers were exposed in the immediate vicinity to the samples (Fig. 1). The concentrations of traffic-generated pollutants, i.e. nitrogen dioxide (NO_2) and ozone (O_3), were monitored on a regular basis using Gradko (Winchester, UK) passive samplers DIF 500 RTU for NO_2 and DIF 300 RTU for O_3. Sulfur dioxide (SO_2) concentrations were not monitored, since in post-industrial environments the concentrations of this pollutant are generally very low and in most of the environments used in this research do not exceed the value of 1 ppb [12], which is commonly the value considered safe for paper collections according to several standards and guidelines [7]. The tubes were exposed next to the samples (Fig. 1) for 4 weeks per monitoring period; the monitoring periods coincided with the first 4 weeks of what was normally a 3-month sample exposure period, and it was assumed that the obtained concentrations were representative of the pollutants concentrations in the respective exposure period as a whole.

2.4 Sampling

The samples were sent from the exposure site to the Heritage Science Laboratory at UCL Institute for Sustainable Heritage, London. The day and time of collection marked the end of the exposure period, after which the samples travelled in unknown conditions (the travel time was typically up to three days using international couriers and hence insignificant relative to the overall duration of the experiment) and were stored at 4 ^{o}C for several weeks, until the day before analysis. The measurements were done at laboratory conditions. The start and the end of each individual period of exposure were recorded so that the exact duration could be calculated, and the analytical results could be normalised to the length of the exposure period.

Similarly, average values of T (°C), RH (%), E_v/d (daily illuminance, lx/day), c_{NO2} (ppb) and c_{O3} (ppb) were calculated for the corresponding period of exposure only. Due to loss of devices or samples during shipment, or due to malfunctioning loggers, the collection of data was suboptimal.

2.5 Colour measurements

Colour of the samples was measured using the CIE 1976 L*a*b* colour space [13] with an X-Rite (Poynton, UK) 500 Series portable spectrodensitometer, and because changes in the yellow-blue coordinate b* are mostly due to chemical factors, e.g. presence of groundwood or optical brighteners in the paper composition, Δb* [14] was calculated. Each colour measurement was performed on a non-printed area, after brushing the sample to remove any deposited particulates. Three measurements were taken and the averages were used for data analysis. The measurements were repeatable to ±0.1 units.

2.6 Degree of polymerisation measurements

Degree of polymerisation (DP) of the samples was measured using capillary viscometry. Since DP measurements could not be carried out on lignin-containing paper, as lignin is insoluble in cupriethylenediamine (CED, i.e. the solvent used in viscometric determination of DP), only DP values of non-groundwood paper were calculated. A 20±1 mg fragment from each alkaline paper sample and a 30±1 mg fragment from each acidic paper sample were produced for viscometry measurements and the exact mass of each fragment was recorded. Each fragment was transferred into a 50 mL glass flask without prior manual shredding, and a small number of copper wires and 10 mL of deionised water were added before sealing the flask tightly. The flasks were then shaken until the samples were homogeneously dispersed. Afterwards, 10 mL of CED (1 mol/L) was added to each sample, flushing the flask with nitrogen before sealing it tightly again. The flasks were placed in a thermostatic chamber at a temperature of 25±0.1 °C for at least 20 min. Four measurements were taken per sample, recording the flowing time of the solution between two reference lines on a glass capillary viscometer. A reference sample (i.e. one glass flask containing a solution of 20 mL of deionised water and 20 mL of CED) was used during the analytical process. Mass and time data for each sample were used for calculation of DP. All the measurement materials were thoroughly cleaned with deionised water, 2-propanol and diluted hydrochloric acid before every analytical sessions.

2.7 Data evaluation

After detecting and removing inaccurate records from the collection of observations, e.g. colour measurements influenced by the presence of dirt, and time measurements affected by random errors, data was divided into two sets: the first set (dataset 1) was used to determine changes in colour (yellowing rate, $\Delta b^*/t$) and included 72 observations (27 containing optical brighteners and 45 without optical brighteners), the second one (dataset 2) was used to determine changes in mechanical properties (rate of change in degree of polymerisation, $\Delta(1/DP)/t$) and included 127 observations. The independent variables, related to both environmental factors (T, RH, E_v/d, c_{NO2} and c_{O3}) and material characteristics (pH, groundwood content –GW– and content of optical brighteners –OB–), chosen for this study are assumed to contain substantial information about paper degradation, as is suggested in chemical literature relevant to this topic. For instance, temperature is recognised as a crucial factor for paper chemical degradation [5,15]; additionally, it is likely that considerable synergistic/antagonistic interactions within environmental variables (e.g. between RH and other environmental variables), as well as between environmental variables and material variables (e.g. between c_{NO2} and GW) exist [8,16-18]. The relationships between independent variables and rate of change (either in colour or DP) were statistically examined using a range of approaches. First of all, a preliminary examination by means of conventional descriptive statistics made it possible to observe potential linear correlations between any independent variables in the datasets. This was repeatedly achieved arranging a number of scatter plots, each of which displayed the correlation between a pair of variables, in a matrix format, i.e. the scatterplot matrix [19]. Subsequently, the datasets were interpreted using multiple linear regression (MLR), which uses several independent variables simultaneously to predict one or more dependent variables, making it possible to develop dose-response functions for future damage modelling [20]. This method also has the potential to highlight independent variables with high statistical significance (i.e. characterised by a p-value less than or equal to a chosen significance level α; in this study $\alpha = 0.05$ was the selected significance level) and possible interactions between such variables. Although MLR is an established method to calculate predictive models, this technique fails if strong linear correlations exist between the independent variables (i.e. multicollinearity), which causes unstable (i.e. not precisely estimated) regression coefficients and inflated standard errors in the models [21,22]. Therefore, to address the problem of multicollinearity, stepwise selection was used to improve the MLR models, by selecting variables at different steps according to certain statistical criteria [23], while principal component regression (PCR) was used to cross-validate MLR models, as it is unaffected by inter-correlated independent variables [24]. Stepwise selection may be applied following two different iterative processes: backward selection, which works by eliminating variables, and forward selection, which, on the other hand, works by adding variables [25]. In this study, only backward stepwise selection was used, starting with an MLR full model, which included all candidate k variables, and then removing each variable one at a time, to create k new models, each one containing $k-1$ variables. By using a comparison criterion, the MLR model that best fitted the population, from which the data were sampled, could be identified among all the available models (i.e. the initial full model and the new models). When the best model was the initial model, meaning that there was no improvement, then the process could be stopped. On the contrary, when the best model was one of the models with variable deletion, then this model could be used as a starting model during the following step in the selection process; this process was repeated until no improvement could be detected. In this work, the criterion chosen to compare the models was the Akaike information criterion (AIC), which was first introduced by Akaike [26] and is commonly used for this purpose. Essentially, as shown in Eq. (1), AIC offers a relative measure of the information lost when a statistical model is used to analyse data, evaluating the fitting power of the model [27]:

$$\mathrm{AIC} = 2k - 2\ln(L) \tag{1}$$

where k indicates the number of variables in the statistical model and L indicates the maximised value of the likelihood function for the model. In backward stepwise selection, AIC was calculated for each candidate model, making it possible to retain the best model characterised by the smallest AIC.

PCR is a multivariate calibration technique that uses the principal components loadings, generated by means of principal component analysis (PCA), to estimate regression coefficients. PCR overcomes the problem of model instability caused by multicollinearity, by calculating the regression coefficients on orthogonally transformed variables (i.e. the principal components or PCs) [28,29]. Since some PCs only contribute to noise due to the lack of sufficient variance and are not useful, PCR typically regresses the response on a limited subset of PCs. Deciding the optimal number of PCs that should be retained in order to explain a high percentage of the variation in the data, and consequently to provide enough information, is crucial to guarantee the stability of the obtained model. Among the different methods to determine a suitable number of variables, in this study a combination of the scree plot rule and the Kaiser criterion was used. The scree plot is a graphical display of the total residual variance of each PC in the dataset, which is used to select the PCs that account for sufficient variance by observing a particular point, called elbow, separating the “steeper” region from the “flatter” region of the trend line; all the PCs before that point (i.e. with higher variance) should be retained, while the other PCs (i.e. with lower variance) should be considered unnecessary and discarded, although in some cases dropping these PCs might lead to ignoring important information [24]. The Kaiser criterion is based on retaining all PCs with variance greater than 1 [30].

3 Results and discussion

3.1 Environmental assessment

Physical environmental variables, i.e. T, RH and E_v, were continuously monitored using data loggers, while the concentrations of traffic-generated pollutants, i.e. NO_2 and O_3, were monitored every three months using passive samplers at the start of each exposure period. The variability of exposure environments at the eleven sites was previously assessed and described in great detail by the authors of this work in another study [12], and can be summarised as follows:

- Variation in temperature: −10 - 50 ºC
- Variation in relative humidity: 10 - 95%
- Variation in illuminance: 0 - 1.2×10^4 lx
- Max NO_2 concentration: 31 ppb
- Max O_3 concentration: 60 ppb

Ranges of environmental values relevant to the two datasets used for this research are presented in Tab. 3 together with other independent and dependent variables values ranges. The measured ranges covered the expected range of climate and pollution level in indoor situations in most museums and archives.

Table 3. Variables contained in colour-change dataset (1) and DP-change dataset (2), and relative ranges of variable values during the entire period of exposure.

Class of variables contained in datasets	Variable	Values range	
		Dataset 1	Dataset 2
Environmental explanatory variables (independent)	Temperature (T)	7.36 - 21.76 °C	7.36 - 28.76 °C
	Relative humidity (RH)	48.57 - 74.24%	37.94 - 73.49%
	Daily illuminance (E_v/d)	0.2×10^4 - 1.60×10^4 lx/day	0.2×10^4 - 1.18×10^4 lx/day
	Concentration of NO_2 (c_{NO2})	4.76 - 24.44 ppb	4.75 - 24.44 ppb
	Concentration of O_3 (c_{O3})	5.48 - 43.99 ppb	5.48 - 43.99 ppb
Material explanatory variables (independent)	pH	4.80 - 8.00	4.80 - 8.00
	Content of lignin (GW)	0 - 0.90%	-
	Content of optical brighteners (OB)	0 (without) or 1 (with)	-
Response variable (dependent)	Degradation rate (Δ/t, t ≈ 3 months)	−0.04 - 0.06	0 - 4.91

3.2 Analytical results

Data obtained from regular assessment of the colour of paper samples using spectrocolorimetry was expressed using the CIE L*a*b* colour space, and the yellow-blue coordinate b* was measured together with the viscometric average DP for each sample after each period of exposure. The difference values Δb* and Δ(1/DP) were calculated for each exposure period and normalised to the length of the period. While the decrease of DP was observed in most of the instances (especially in alkaline paper samples due to the fact that the average molecular weight of acidic paper samples was already significantly low at the beginning of the experiment), results suggested that different types of paper yellowed (or bleached) very differently in the same environmental conditions. As an example, Fig. 2 shows that for contemporary alkaline papers with photo-unstable bleached pulp content, as well as presence of optical brighteners, yellowness tended to increase, while, on the other hand, for historic acidic papers with no optical brightener content yellowness tended to decrease.

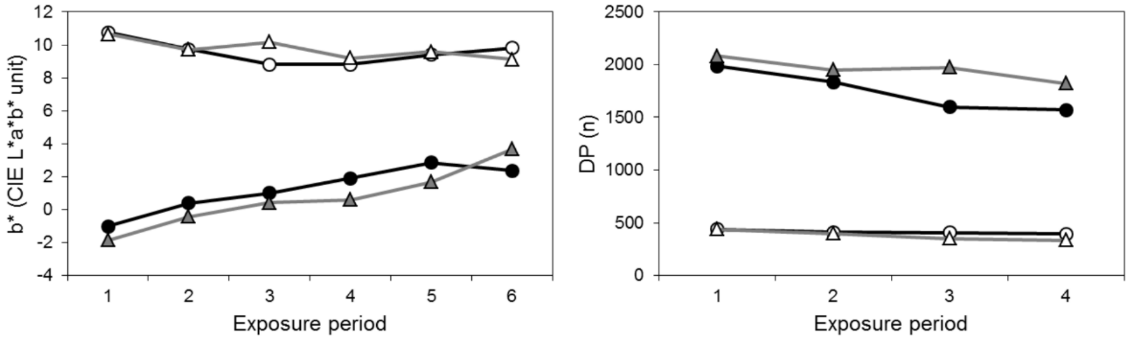

Figure 2. Variation of the yellow-blue coordinate b* (left) and DP (right) for two different types of paper (empty symbols – acidic without optical brighteners; filled symbols – alkaline with optical brighteners) exposed to two different sites (circles – environment 1; triangles – environment 2) after 1.5-year and 1-year outdoor exposure respectively.

3.3 Calculation of the dose-response function for colour change

Colour results were used to calculate the rate of yellowing ($\Delta b^*/t$), which was subsequently used for calculation of the dose-response function. As seen in Table 3, the values of independent variables, both environmental and material, in dataset 1 covered relatively large ranges. However, the sample distributions of those variables presented different trends, as shown by the scatterplot matrix in Fig. 3. Specifically, T and E_v/d were characterised by bell-shaped, i.e. unimodal, distributions; c_{NO2}, c_{O3} and pH showed bimodal distributions; the distribution of RH was nearly uniform; most values of GW were extremely small, i.e. close to 0%. In the same scatterplot matrix, a few linear correlations between some independent variables can be appreciated, e.g. a negative correlation between T and RH and positive correlations between RH and E_v/d, between E_v/d and c_{O3}, and between pH and OB. These linear correlations indicate the presence of multicollinearity in the dataset, which could represent a major problem for MLR interpretation. In fact, the initial MLR model (i.e. the full model including all variables) showed p-values greater than 0.05 for all the independent variables except pH and GW only (Tab. 4). Since the large p-values could be caused by multicollinearity, backward stepwise variable selection based on AIC was used to analyse the data further. At the end of the process, a model only including the three material variables was obtained (Tab. 4). In this new model pH and GW maintained their significance, while OB was associated with a p-value equal to 0.08, which could be caused by the strong linear correlation between pH and OB observed previously. According to Porck [31], papers with and without optical brightener content may be characterised by different major degradation mechanisms, besides, the former tend to have a higher degradation rate. Supposing that the effects of the other explanatory variables can change depending on the two different values (0 or 1) of the variable OB, the dataset was divided into two sub-datasets, one identified by the presence of optical brighteners (sub-dataset OB1) and one by their absence (sub-dataset OB0), which were analysed separately. In order to verify the previous assumptions and support further analyses, a new scatterplot matrix, with two colours to show the different data points from the two sub-datasets, was produced (Fig. 4). As shown by the matrix, significant differences in average values and regression lines slopes between the two groups of data can be observed. In particular, the response values in the OB1 sub-dataset are generally higher than the ones in the OB0 sub-dataset. Hence, separate variable selection processes were performed with the two groups of data.

Regarding the OB1 sub-dataset, after using backward stepwise variable selection based on AIC, the remaining variables in the final MLR model were T, c_{O3}, pH and GW (Tab. 5). This model indicated that T was characterised by a p-value greater than 0.05, suggesting low significance. However, it is well known that temperature plays an important role in chemical degradation of paper [5,15]. Thus, the model was developed further, taking into account possible interactions between the independent variables, both included and not included in the model, e.g. between c_{NO2} and GW [16] and between RH and other variables [17,18], possibly leading to a more significant involvement of T. After a number of interaction trials within the model, a new model also including the variables RH and c_{NO2}, and the interactions between c_{O3} and pH (c_{O3}*pH), and between c_{NO2} and GW (c_{NO2}*GW) was obtained (Tab. 5). Although the p-value of pH resulted much larger than its counterpart in the model without the interaction terms, the p-value of T resulted much smaller than the previous value and all the additional variables and interactions also resulted significant. Therefore, this model was chosen to be the final model for the OB1 sub-dataset and could be expressed using the following Eq. (2):

$$y_i^{\Delta b^*} = \alpha_0 + \alpha_1 X_i^{T} + \alpha_2 X_i^{RH} + \alpha_3 X_i^{cNO_2} + \alpha_4 X_i^{cO_3} + \alpha_5 X_i^{pH} + \alpha_6 X_i^{GW} + \alpha_7 X_i^{cO_3} X_i^{pH} + \alpha_8 X_i^{cNO_2} X_i^{GW} + \epsilon_i \quad (2)$$

where $y_i^{\Delta b^*}$ is the ith response value of the yellowing rate, X_i is the ith observation (which includes six variables) and ϵ_i is the error term. This model was characterised by a high power of explanation ($R^2 = 81\%$) and led to interesting findings about NO_2 and O_3. Specifically, NO_2 has positive effects on the degradation rate, meaning that this pollutant could accelerate the yellowing process in paper with optical brighteners. In contrast, high concentrations of O_3 appear to slow down the yellowing process, possibly because ozone is a powerful oxidant and may act as a bleaching agent. Regarding the interaction effects of these pollutants, concentration of NO_2 and groundwood content seem to have antagonistic effects, while concentration of O_3 and pH seem to have synergistic effects. These complex interactions may be explained by assuming the occurrence of different degradation mechanisms competing with each other. For instance, both high NO_2 concentration and high groundwood content could intensify degradation, but an antagonistic interaction between them could make one mechanism overcome the other. A similar competition between O_3 concentration and pH, which have opposite effects, could result in analogous outcomes: mechanisms promoted by high pH could prevail over reactions with O_3, decreasing the mitigation effect of the latter. Interestingly, high temperature and relative humidity seem to slow down the degradation process, which may contradict previous work based on accelerated and natural degradation tests [32]. However, as noted by Kolar et al. [33], colour reversion may happen during periods in darkness; thus, the observed unusual effect of temperature could be a consequence of two competing processes, yellowing and bleaching, which are differently promoted by light during exposure and absence of light during night-time, shipping and storage before colour analysis. Moreover, although the water content of paper promotes mobility of reactive species that cause paper degradation [5], at RH > 80% the saturation of the material with water possibly leads to lower diffusion of oxygen [18], decreasing the rate of degradation. Concerning the OB0 sub-dataset, after using backward stepwise variable selection based on AIC, the remaining variables in the final MLR model were E_v/d, pH and GW (Tab. 6), showing evident differences with the OB1 sub-dataset. This model indicated that all variables were characterised by a high significance. However, since other variables such as T, RH, c_{NO2} and c_{O3}, as already seen, play important roles in chemical degradation of paper, some interactions between the variables included in the obtained model and those variables that are not included were considered possible. After a number of interaction trials, no significant result was found. Therefore, the model was chosen to be the final model for the OB0 sub-dataset and could be expressed using the following Eq. (3):

$$y_i^{\Delta b^*} = \alpha_0 + \alpha_1 X_i^{Ev/d} + \alpha_2 X_i^{pH} + \alpha_3 X_i^{GW} + \epsilon_i \tag{3}$$

where $y_i^{\Delta b^*}$ is the *i*th response value of the yellowing rate, X_i is the *i*th observation (which includes three variables) and ϵ_i is the error term. The interpretation of this model appears more challenging than the previous one, due to the uncertain effect of light and the relatively low power of explanation ($R^2 = 54\%$), which suggests the potential presence of latent degradation mechanisms not modelled by linear relationships. However, high pH and high groundwood content seem to accelerate the degradation rate in paper without optical brighteners.

These statistical results indicate different major degradation mechanisms for paper with and without optical brighteners: paper samples with optical brighteners appear more sensitive to environmental factors such as temperature, humidity and pollutants, and more prone to yellowing, whereas paper samples without optical brighteners seem to be more sensitive to light and more prone to bleaching. Additionally, it is worth mentioning that photochemical reactions between NO_2 and oxygen lead to the formation of O_3 [8], as confirmed by the positive linear correlation between E_v/d and c_{O3}. Although the environmental variables c_{O3} and E_v/d play important roles in the presence and in the absence of optical brighteners respectively, the obtained results did not clarify whether it may be E_v/d or c_{O3} having a direct effect on paper degradation.

The MLR models for colour-change were validated by means of PCR. Details about the methodology and the results are provided in the supplementary document *Model validation by principal component regression*.

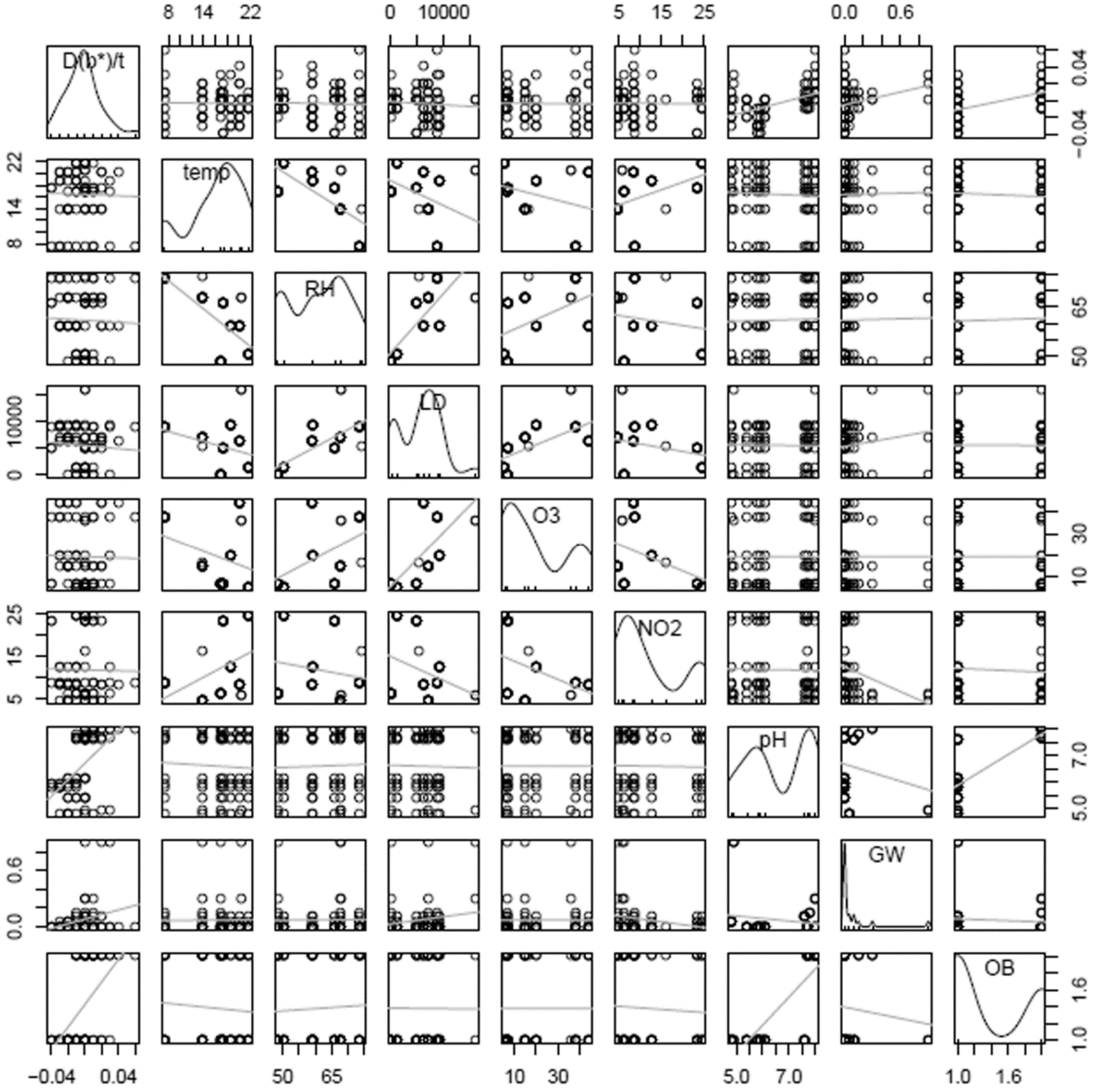

Figure 3. Scatterplot matrix of dataset 1 (colour-change).

Table 4. MLR statistics of dataset 1 (colour-change). Positive (+) and negative (−) signs before the estimate values indicate a positive and a negative effect of the variables respectively. Errors, which represent standard errors, and *p*-values are expressed with one significant figure. The *p*-values of significant variables (≤ 0.05) are indicated in bold.

Variable		Initial model		Final model	
		Estimate	*p*-value	Estimate	*p*-value
Env.	T	− 0.0006 ± 0.0008	0.5		
	RH	− 0.0002 ± 0.0006	0.7		
	E_v/d	0	0.4		
	c_{NO2}	+ 0.0005 ± 0.0004	0.2		
	c_{O3}	+ 0.0002 ± 0.0002	0.2		
Mat.	pH	+ 0.005 ± 0.003	**0.04**	+ 0.005 ± 0.003	**0.04**
	GW	+ 0.04 ± 0.01	**0.0002**	+ 0.03 ± 0.01	**0.0008**
	OB	+ 0.012 ± 0.006	0.07	+ 0.011 ± 0.006	0.08

Env.: environmental variables; Mat.: material variables.

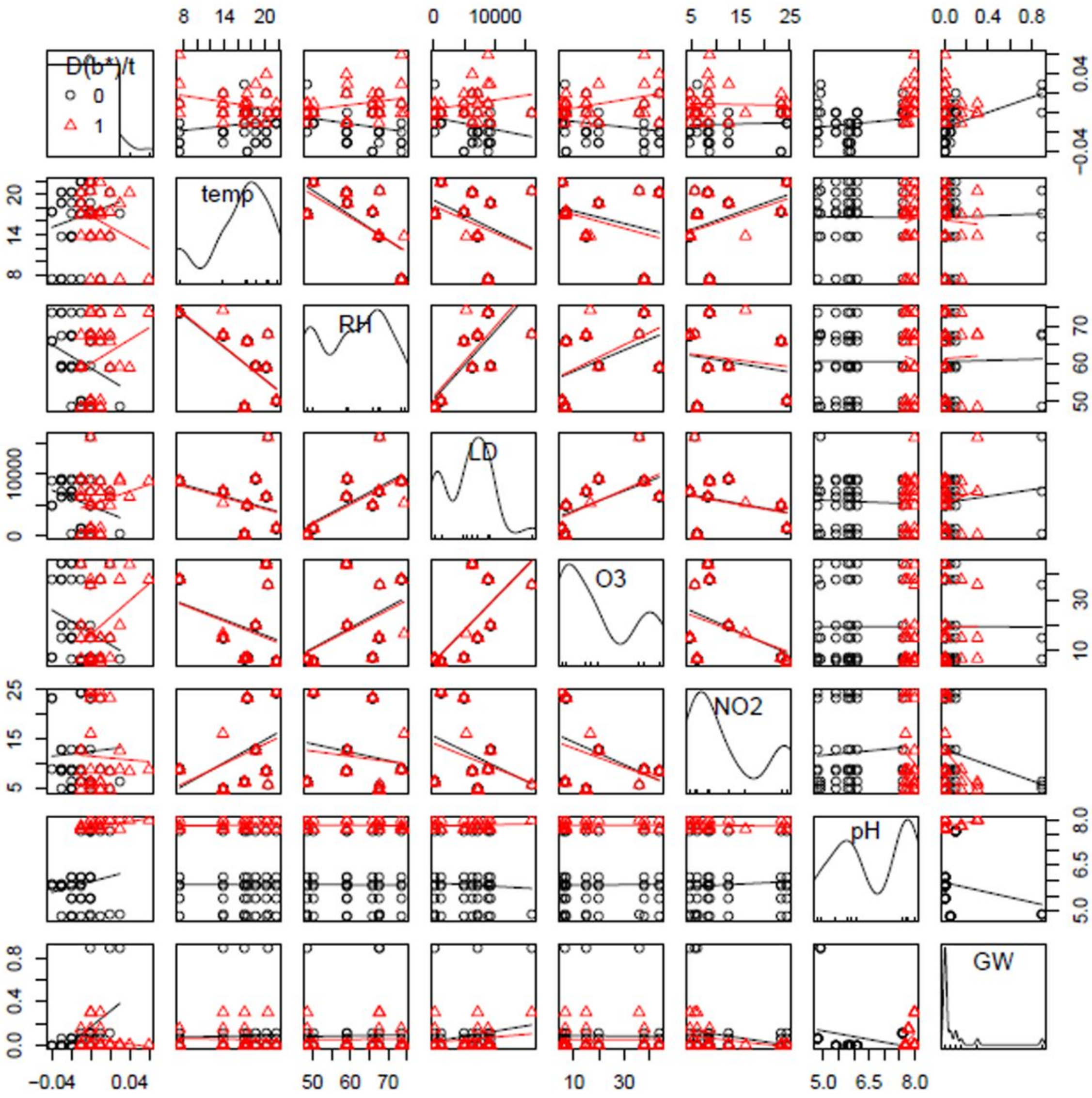

Figure 4. Scatterplot matrix of sub-dataset OB1 (colour-change in relation to the presence of optical brighteners - red) and sub-dataset OB0 (colour-change in relation to the absence of optical brighteners - black).

Table 5. MLR statistics of sub-dataset OB1 (colour-change in the presence of optical brighteners). Positive (+) and negative (−) signs before the estimate values indicate a positive and a negative effect of the variables/interactions respectively. Errors, which represent standard errors, and *p*-values are expressed with one significant figure. The *p*-values of significant variables and interactions (≤ 0.05) are indicated in bold.

Variable		Model without interaction terms		Model with interaction terms	
		Estimate	*p*-value	Estimate	*p*-value
Env.	*T*	− 0.0010 ± 0.0005	0.06	− 0.0026 ± 0.0007	**0.002**
	RH			− 0.0007 ± 0.0003	**0.05**
	c_{NO2}			+ 0.0008 ± 0.0003	**0.04**
	c_{O3}	+ 0.0003 ± 0.0002	**0.04**	− 0.016 ± 0.007	**0.03**
Mat.	pH	+ 0.08 ± 0.02	**0**	+ 0.04 ± 0.02	0.09
	GW	− 0.08 ± 0.02	**0.001**	+ 0.2 ± 0.1	**0.05**
Int.	c_{O3}*pH			+ 0.0021 ± 0.0009	**0.02**
	c_{NO2}*GW			− 0.05 ± 0.02	**0.01**

Int.: interactions.

Table 6. MLR statistics of sub-dataset OB0 (colour-change in the absence of optical brighteners). Positive (+) and negative (−) signs before the estimate values indicate a positive and a negative effect of the variables respectively. Errors, which represent standard errors, and *p*-values are expressed with one significant figure. The *p*-values of significant variables (≤ 0.05) are indicated in bold.

Variable		Estimate	*p*-value
Env.	E_v/d	0	**0.002**
Mat.	pH	+ 0.005 ± 0.002	**0.02**
	GW	+ 0.047 ± 0.008	**0**

3.3 Calculation of the dose-response function for DP change

Similarly to dataset 1 for colour change, dataset 2 was characterised by wide ranges of data values (Tab. 3), in addition to distinctive distributions, as shown by the scatterplot matrix in Fig. 5. The environmental variable T showed unimodal distribution, while most of the other variables, i.e. RH, E_v/d, c_{NO2}, c_{O3} and pH, tended to have bimodal distributions with different degrees of skewness and kurtosis. In the scatterplot matrix, a few linear correlations between some independent variables can also be appreciated, e.g. negative correlations between T and RH, between E_v/d and c_{NO2}, and between c_{NO2} and c_{O3}, and positive correlations between RH and E_v/d, and between E_v/d and c_{O3}. Also in this case, such linear correlations indicate the presence of multicollinearity in the dataset, which could represent a major problem for MLR interpretation. In fact, a pilot MLR model (including all variables) showed p-values larger than 0.05 for all the variables except c_{O3} and pH. Hence, backward stepwise variable selection based on AIC was used to analyse the data further. At the end of the process, a model only including T, c_{O3} and pH was obtained (Tab. 7). Similarly to the colour-change dataset, some interactions between variables, both included and not included in the model, were considered and, after a number of interaction trials within the model, the interactions between T and c_{NO2} (T*c_{NO2}), RH and E_v/d (RH*E_v/d), and c_{O3} and pH (c_{O3}*pH) were found to be significant (Tab. 7). Although the variables T and pH showed very low significance, this model was chosen for dataset 2, due to the previously observed importance of these variables, and could be expressed using the following Eq. (4):

$$y_i^{\Delta\frac{1}{\mathrm{DP}}} = \alpha_0 + \alpha_1 X_i^{T} + \alpha_2 X_i^{RH} + \alpha_3 X_i^{Ev/d} + \alpha_4 X_i^{cNO_2} + \alpha_5 X_i^{cO_3} + \alpha_6 X_i^{pH} + \alpha_7 X_i^{T} X_i^{cNO_2} + \alpha_8 X_i^{RH} X_i^{Ev/d} + \alpha_9 X_i^{cO_3} X_i^{pH} + \epsilon_i \tag{4}$$

where $y_i^{\Delta 1/\mathrm{DP}}$ is the ith response value of the DP-change rate, X_i is the ith observation (which includes six variables) and ϵ_i is the error term. Although all the available variables were used, this model was characterised by a low power of explanation (R^2 = 46%), which means that some latent degradation mechanisms or factors may need to be explored. High temperature and NO_2 concentration accelerate degradation, even though the effect of c_{NO2} could be more important than that of T (as shown by their respective p-values). However, due to the interaction between T and c_{NO2}, high levels of temperature and NO_2 concentration tend to decrease the acceleration effect, which indicates an antagonistic interaction. Additionally, high levels of relative humidity and daily illuminance tend to slow down the degradation rate, but their interaction seems antagonistic and able to nullify the effects of both factors. Also, high pH and high O_3 concentration have opposite effects, i.e. slowing down and accelerating degradation respectively. On the other hand, degradation mechanisms due to high pH can prevail on mechanisms due to high O_3 concentrations, moderating the accelerating effect of the latter. This antagonistic interaction between pH and c_{O3} is similar, but with opposite effects, to the one described in the interpretation of the colour-change model in the presence of optical brighteners.

The MLR model for DP-change was validated by means of PCR. Details about the methodology and the results are provided in the supplementary document *Model validation by principal component regression*.

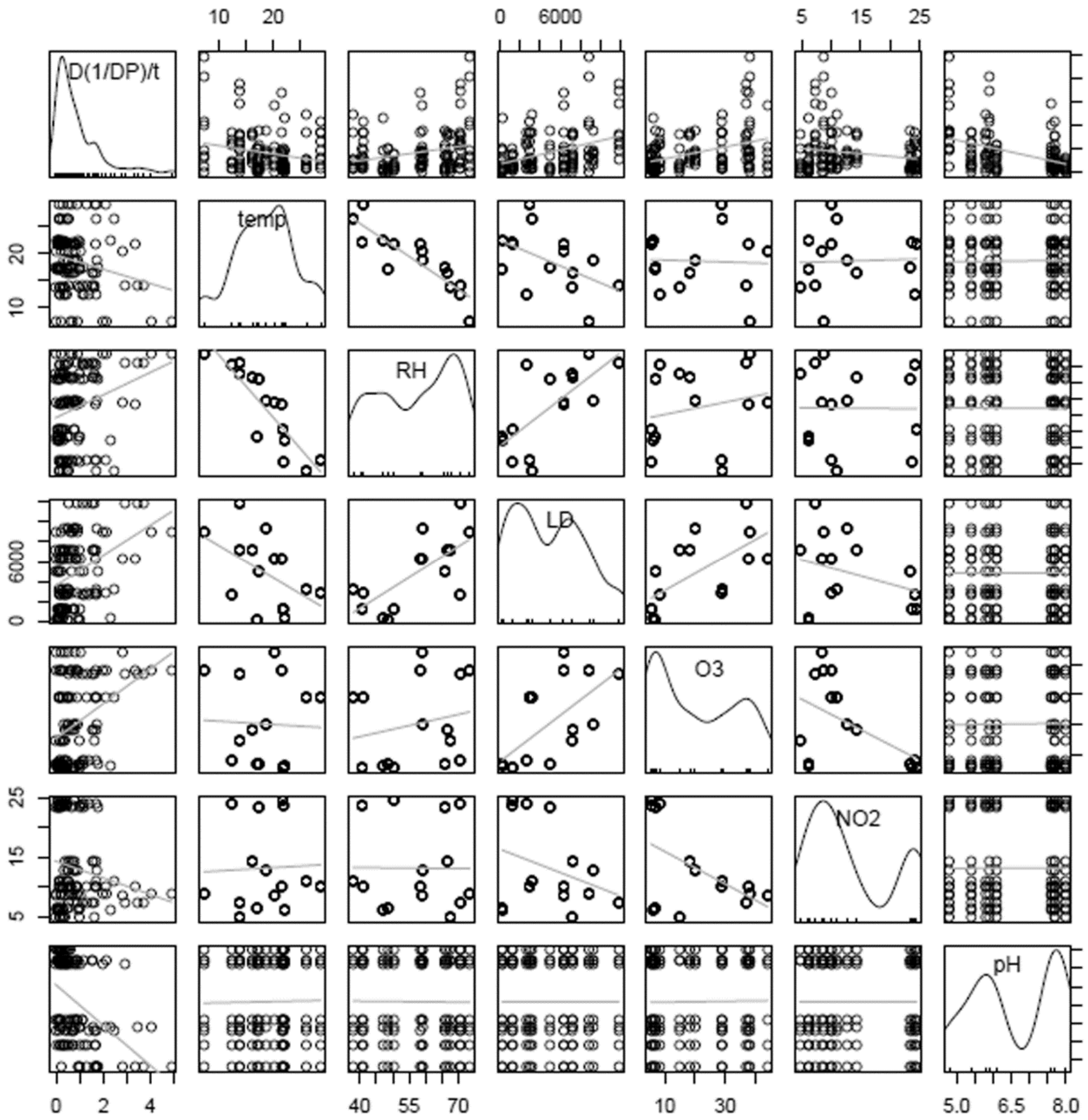

Figure 5. Scatterplot matrix of dataset 2 (DP-change).

Table 7. MLR statistics of dataset 2 (DP-change). Positive (+) and negative (−) signs before the estimate values indicate a positive and a negative effect of the variables/interactions respectively. Errors, which represent standard errors, and *p*-values are expressed with one significant figure. The *p*-values of significant variables and interactions (≤ 0.05) are indicated in bold.

Variable		Model without interaction terms		Model with interaction terms	
		Estimate	*p*-value	Estimate	*p*-value
Env.	T	− 0.03 ± 0.01	**0.008**	+ 0.07 ± 0.04	0.08
	RH			− 0.04 ± 0.02	**0.05**
	E_v/d			− 0.0006 ± 0.0002	**0.005**
	c_{NO2}			+ 0.13 ± 0.06	**0.02**
	c_{O3}	+ 0.09 ± 0.03	**0.002**	+ 0.08 ± 0.03	**0.004**
Mat.	pH	− 0.1 ± 0.1	0.1	− 0.2 ± 0.1	0.1
Int.	T*c_{NO2}			− 0.006 ± 0.003	**0.03**
	RH*E_v/d			0	**0.002**
	c_{O3}*pH			− 0.009 ± 0.004	**0.03**

4 Conclusions

The aim of this study was to develop a novel methodology to calculate dose-response functions, by applying an experimental approach based on moderate acceleration in conjunction with advanced statistical techniques. Although the experimental times are long, it could be argued that the obtained results can be more reliably extrapolated to real conditions; however, data analysis revealed several methodological challenges. In our research we explored quantitative analysis of comprehensive environmental and material datasets, which included a wide range of variables with potentially high influence in dose-response functions. The results of this study, therefore, complement other current research, provide a more complex view of paper degradation, and stress important gaps in knowledge such as variable interactions and the influence of light/dark cycles.

Advanced statistical methods, i.e. stepwise selection MLR and PCR, were used to address the problem of multicollinearity. From MLR models of two datasets, one for rate of colour change and one for rate of DP change, it was found that all the considered variables, related to both the environment and the paper material, are of significance. Additionally, some meaningful interactions between those variables were revealed, which is an important finding. For colour-change, the presence of optical brighteners led to a higher rate of yellowing, compared to paper without optical brighteners. After separation of the data into two groups and stepwise selection MLR on each group, two distinct models were created. The model related to paper samples containing optical brighteners showed a high sensitivity to environmental variables, such as temperature, RH and concentrations of NO_2 and O_3, as well as to the two available material variables, i.e. pH and groundwood content, and was characterised by a high power of explanation. The model related to samples without optical brighteners was only sensitive to one environmental variable, i.e. daily illuminance, as well as to the two available material variables, i.e. pH and groundwood content, and its power of explanation was weaker compared to the previous model. The MLR model regarding the DP-change dataset included all the available variables, i.e. temperature, RH, daily illuminance, concentrations of NO_2 and O_3, and pH, but the power of explanation was also relatively low. Most of the findings obtained by PCR were consistent with the MLR results and some interesting supplementary details were revealed. Specifically, a number of underlying patterns, which could not be detected by MLR, were discovered, such as the effects of temperature, RH and concentrations of NO_2 and O_3 in colour-change data in the absence of optical brighteners.

This experimental approach to accelerated degradation of real (i.e. not model) samples could find more widespread use in heritage science in the future; however, great care must be taken to ensure that the spread of data (both material and environmental) is appropriate and that the data is as accurate as possible. There is no other experimental approach currently available that would explore the effect of a multitude of degradation variables simultaneously, which is extremely important for informed preventive conservation of cultural heritage.

Acknowledgements

The authors are grateful to Linda Cséfalvayová for technical assistance with the experiments during the course of this research, and to paper conservation experts at the Royal Danish Library and the National Gallery of Denmark, in particular Birgit Vinther Hansen, Niels Borring and Kathleen Mühlen Axelsson, for their valuable insights. The authors gratefully acknowledge funding from the European Commission 7th Framework Programme (grant number 212458, TEACH–Technologies and Tools to prioritize assessment and diagnosis of air pollution impact on immovable and movable Cultural Heritage) and Research Programme P1-0153 funded by the Research Agency of the Republic of Slovenia.

References

1. Strlič M, Kolar J, Scholten S. Paper and durability. In: Strlič M, Kolar J, editors. Ageing and stabilisation of paper. Ljubljana, Slovenia: Narodna in univerzitetna knjižnica; 2005.

2. Zou X, Gurnagul N, Uesaka T, Bouchard J. Accelerated aging of papers of pure cellulose: mechanism of cellulose degradation and paper embrittlement. Polym Degrad Stabil 1994;43:393-402.

3. Zou X, Uesaka T, Gurnagul N. Prediction of paper permanence by accelerated aging I. Kinetic analysis of the aging process. Cellulose 1996;3:243-267.

4. Shahani CJ, Harrison G. Spontaneous Formation of Acids in the Natural Aging of Paper. In: Works of Art on Paper: Books, Documents and Photographs. Edited by Daniels V, Donnithorne A, and Smith P, 189-192. London: International Institute for Conservation of Historic and Artistic Works; 2002.

5. Calvini P, Gorassini A. On the rate of paper degradation: lessons from the past. Restaurator 2006;27(4):275-290.

6. Menart E, de Bruin G, Strlič M. Effects of NO_2 and acetic acid on the stability of historic paper. Cellulose. 2014;21(5):3701-13.

7. Di Pietro G, Ligterink F, Porck H, de Bruin G. Chemical air filtration in archives and libraries reconsidered. Stud Conserv. 2016;61(5):245-54.

8. Menart E, De Bruin G, Strlič M. Dose-response functions for historic paper. Polym Degrad Stabil 2011;96(12):2029-2039.

9. Strlič M, Grossi CM, Dillon C, Bell N, Fouseki K, Brimblecombe P, Menart E, Ntanos K, Lindsay W, Thickett D, France F, De Bruin G. Damage function for historic paper. Part I: Fitness for use. Heritage Science 2015;3:33.

10. Strlič M, Grossi CM, Dillon C, Bell N, Fouseki K, Brimblecombe P, Menart E, Ntanos K, Lindsay W, Thickett D, France F, De Bruin G. Damage function for historic paper. Part II: Wear and tear. Heritage Science 2015;3:36.

11. Strlič M, Grossi CM, Dillon C, Bell N, Fouseki K, Brimblecombe P, Menart E, Ntanos K, Lindsay W, Thickett D, France F, De Bruin G. Damage function for historic paper. Part III: Isochrones and demography of collections. Heritage Science 2015;3:40.

12. Pastorelli G, Cucci C, Garcia O, Piantanida G, Elnaggar A, Cassar M, Strlič M. Environmentally induced colour change during natural degradation of selected polymers. Polym Degrad Stabil 2013;107:198-209.

13. Commission Internationale de l’Éclairage (CIE). Colorimetry - Part 4: CIE 1976 L*a*b* colour space (ISO 11664-4:2008(E)/CIE S 014-4/E:2007), 2008. Retrieved from http://www.cie.co.at/publications/colorimetry-part-4-cie-1976-lab-colour-space.

14. Robertson AR. Historical development of CIE recommended color difference equations. Color Res Appl 1990;15:167-170.

15. Strang T, Grattan D. Temperature and humidity considerations for the preservation of organic collections - the isoperm revisited. e-PS 2009;6:122-128.

16. Brimblecombe P. The composition of museum atmospheres. Atmos Environ B-Urb 1990;24(1):1-8.

17. Havermans JB. Effects of air pollutants on the accelerated ageing of cellulose-based materials. Restaurator 1995;16(4):209-233.

18. Kocar D, Strlič M, Kolar J, Rychly L, Matisovo-Rychlo L, Pihlar B. Chemiluminescence from paper III: the effect of superoxide anion and water. Polym Degrad Stabil 2005;88(3):407-414.

19. Cleveland WS, McGill ME. Dynamic graphics for statistics. Monterey, CA: Wadsworth, 1998.

20. Walker HM, Lev J. Elementary statistical methods. New York: Holt Rinehart and Winston, 1969.

21. Farrar DE, Glauber RR. Multicollinearity in regression analysis: the problem revisited. Rev Econ Stat 1967;49(1):92-107.

22. Haitovsky Y. Multicollinearity in regression analysis: comment. Rev Econ Stat 1969;51(4):486-489.

23. Johnson RA, Wichern DW. Applied multivariate statistical analysis, 5th ed. Upper Saddle River, NJ: Prentice Hall, 2002.

24. Esbensen KH, Guyot D, Westad F, Houmoller LP. Multivariate data analysis - in practice: an introduction to multivariate data analysis and experimental design, 5th ed. Oslo: CAMO, 2002.

25. Derksen S, Keselman HJ. Backward, forward and stepwise automated subset selection algorithms: frequency of obtaining authentic and noise variables. Brit J Math Stat Psy 1992;45(2):265-282.

26. Akaike H. A new look at the statistical model identification. IEEE T Automat Contr 1974;19(6):716-723.

27. Li Z, Tirachini A, Hensher DA. Embedding risk attitudes in a scheduling model: application to the study of commuting departure time. Transport Sci 2012;46(2):170-188.

28. Jolliffe IT. Principal component analysis, 2nd ed. New York: Springer, 2002.

29. Lattin JM, Carroll JD, Green PE. Analyzing multivariate data. Pacific Grove, CA: Thomson Brooks/Cole, 2003.

30. Kaiser HF. The application of electronic computers to factor analysis. Educ Psychol Meas 1960;20:141-151.

31. Porck HJ. Rate of paper degradation: the predictive value of artificial ageing tests. Report. Amsterdam: European Commission on Preservation and Access, 2000.

32. Zou X, Uesaka T, Gurnagul N. Prediction of paper permanence by accelerated aging II. Comparison of the predictions with natural aging results. Cellulose 1996;3(1):269-279.

33. Kolar J, Strlič M, Malesic J, Lemaire J, Fromageot D. Photooxidative degradation. In: Strlič M, Kolar J. editors. Ageing and stabilisation of paper. Ljubljana: National and University Library of Slovenia, 2005. p. 137.

SUPPLEMENTARY MATERIAL

Published in *Polymer Degradation and Stability* 168 (2019) 108944

Model validation by principal component regression

Gianluca Pastorelli, Shuo Cao, Irena Kralj Cigić, Costanza Cucci, Abdelrazek Elnaggar, Matija Strlič

The material contained in this document is supplementary to the article *Development of dose-response functions for historic paper degradation using exposure to natural conditions and multivariate regression*.

1. Validation of the MLR models for colour change

PCR was performed by means of PCA including all the independent variables and after standardisation of the dataset. According to the scree plot/Kaiser rule, the first three PCs, which account for 73% of variance, were suitable for conducting the analysis (Fig. 1).

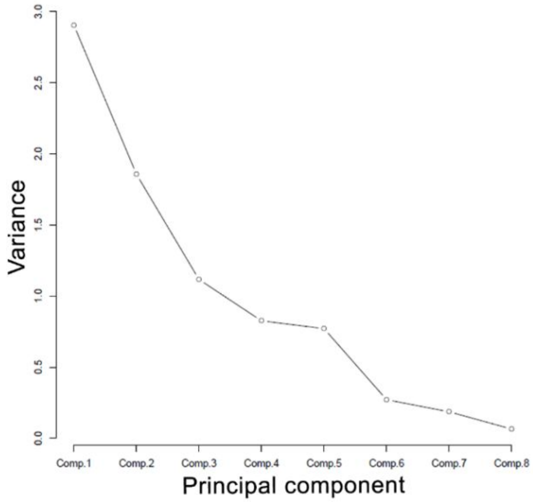

Figure 1. Scree plot of dataset 1 (colour-change).

The resulting loadings (Tab. 1) showed that PC1 was significantly correlated to the environmental variables, while PC2 was significantly correlated to the material variables. In addition, PC3 had significant correlations with c_{NO2} and GW, reflecting the c_{NO2}*GW interaction found with MLR.

Table 1. Loadings for the PCA of dataset 1 (colour-change).

Variable		Loadings		
		PC1	PC2	PC3
Env.	T	0.434		
	RH	−0.508		−0.293
	E_v/d	−0.494		
	c_{NO2}	0.326		−0.551
	c_{O3}	−0.441		
Mat.	pH		0.691	
	GW		−0.228	0.774
	OB		0.679	0.175

To perform PCR, $\Delta b^*/t$ was regressed against the first three PCs. In the obtained model (Tab. 2) PC1 showed a *p*-value equal to 1, while PC2, PC3 and the PC1*PC2 interaction term were all significant, suggesting that degradation mechanisms were associated with both environmental and material variables, but the effects of environmental variables were dependent on material variables.

Table 2. PCR statistics of dataset 1 (colour-change). Positive (+) and negative (−) signs before the estimate values indicate a positive and a negative effect of the principal components/interactions respectively. Errors, which represent standard errors, and *p*-values are expressed with one significant figure. The *p*-values of significant principal components and interactions (≤ 0.05) are indicated in bold.

Principal component	Estimate				*p*-value
PC1		0	±	0.001	1
PC2	−	0.006	±	0.001	**0**
PC3	−	0.007	±	0.002	**0.0002**
PC1*PC2	−	0.0023	±	0.0008	**0.004**

During the MLR analysis, in order to provide more compelling results, the dataset was separated into the two sub-datasets OB1 and OB0. Hence, the same kind of analysis was repeated using PCR (Tab. 3).

Table 3. Loadings for the PCA of sub-dataset OB1 (colour-change in the presence of optical brighteners) and sub-dataset OB0 (colour-change in the absence of optical brighteners).

Variable		OB1 loadings			OB0 loadings		
		PC1	PC2	PC3	PC1	PC2	PC3
Env.	T	0.423	−0.145	−0.448	0.434	−0.153	
	RH	−0.500	0.246	−0.169	−0.505	0.194	−0.345
	E_v/d	−0.501		−0.411	−0.492		−0.246
	c_{NO2}	0.315	0.357	−0.615	0.340	0.303	−0.659
	c_{O3}	−0.445		−0.169	−0.436		0.130
Mat.	pH		−0.599	−0.437		0.597	0.590
	GW	−0.141	−0.650			−0.700	0.140

Generally, PC1 was still correlated to the environmental variables in both groups, while PC2’s and PC3’s correlations were mixed, resulting in a challenging interpretation, although those correlations could reflect degradation mechanisms that are caused by various interactions between environmental and material variables (see references 8,16-18 in the main manuscript). PCR on OB1 resulted in a very complex model which showed the significance of PC3 and the interaction between all three PCs (Tab. 4). The interpretation of this model on the sole base of regression estimation values appeared very challenging; however, the model might provide some interesting information for further research in complex degradation mechanisms of paper.

Table 4. PCR statistics of sub-dataset OB1 (colour-change in the presence of optical brighteners) and sub-dataset OB0 (colour-change in the absence of optical brighteners). Positive (+) and negative (−) signs before the estimate values indicate a positive and a negative effect of the principal components/interactions respectively. Errors, which represent standard errors, and *p*-values are expressed with one significant figure. The *p*-values of significant principal components and interactions (≤ 0.05) are indicated in bold.

Principal component	OB1 final model		OB0 final model	
	Estimate	*p*-value	Estimate	*p*-value
PC1	+ 0.004 ± 0.002	0.09	− 0.002 ± 0.001	0.09
PC2	+ 0.001 ± 0.003	0.7	− 0.006 ± 0.002	**0.005**
PC3	− 0.011 ± 0.004	**0.01**	− 0.008 ± 0.002	**0.005**
PC1*PC2	− 0.003 ± 0.002	0.09		
PC1*PC3	− 0.004 ± 0.002	0.1	− 0.004 ± 0.002	**0.03**
PC2*PC3	− 0.001 ± 0.004	0.8		
PC1*PC2*PC3	+ 0.004 ± 0.002	**0.03**		

PCR on OB0 showed the significance of PC2 and PC3 and a useful interaction between PC1 and PC3 (Tab. 4). This model represented an optimal supplement to the results obtained by MLR analysis, which did not include T, RH, c_{NO2} and c_{O3}. The influence of those important factors was revealed thanks to the application of PCR and their absence in the MLR model could be explained by assuming the existence of some complex underlying patterns, which were impossible to be modelled by linear regression, confirming that PCR can recover useful information potentially missed by MLR. This also explained the low R^2 of the MLR model, since those latent mechanisms could not be modelled.

2. Validation of the MLR model for DP change

PCR was performed by means of PCA including all the independent variables and after standardisation of the dataset. According to the scree plot/Kaiser rule, the first three PCs, which account for 86% of variance, were suitable for conducting the analysis (Fig. 2).

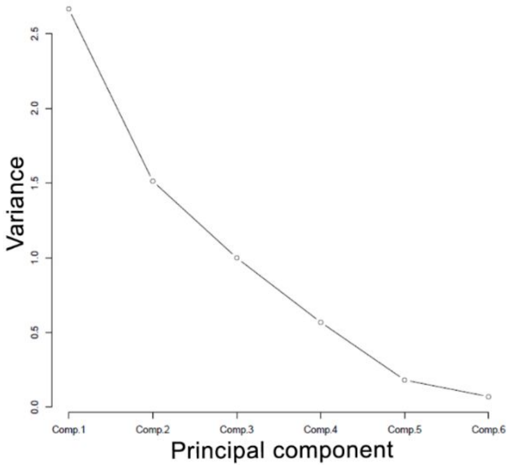

Figure 2. Scree plot of dataset 2 (DP-change).

The resulting loadings (Tab. 5) showed that PC1 was significantly correlated to the physical environmental variables (T, RH and E_v/d), while PC2 was significantly correlated to the chemical environmental variables under the effect of temperature (T, c_{O3} and c_{NO2}). In addition, PC3 had a significant correlation with the material variables only due to the high loading of pH (0.999).

Table 5. Loadings for the PCA of dataset 2 (DP-change).

Variable		Loadings		
		PC1	PC2	PC3
Env.	T	0.461	−0.450	
	RH	−0.527	0.381	
	E_v/d	−0.556	−0.110	
	c_{NO2}	0.243	0.585	
	c_{O3}	−0.376	−0.545	
Mat.	pH			0.999

To perform PCR, Δ(1/DP)/t was regressed against the first three PCs. In the obtained model (Tab. 6) PC2 showed a *p*-value larger than 0.05, while PC2 and PC3 were significant.

Table 6. PCR statistics of dataset 2 (DP-change). Positive (+) and negative (−) signs before the estimate values indicate a positive and a negative effect of the principal components respectively. Errors, which represent standard errors, and *p*-values are expressed with one significant figure. The *p*-values of significant principal components (≤ 0.05) are indicated in bold.

Principal component	Estimate				*p*-value
PC1	−	0.22	±	0.04	**0**
PC2	−	0.08	±	0.05	0.1
PC3	+	0.39	±	0.06	**0**

Hence, to find a suitable model with a high explanation power, an attempt to determine useful interactions between those three PCs was carried out. However, no significant interaction could be found, suggesting that the degradation mechanisms involving *T*, RH, E_v/d and pH were the most prominent. The insignificance of PC2 may be explained assuming that there might be different degradation mechanisms for different pollutants, i.e. NO_2 and O_3. Therefore, the degradation mechanisms caused by those two pollutants might be independent, which is consistent with the different mechanisms shown by the MLR model.

3. Model validation improvements for future studies

Both MLR and PCR have their own advantages and disadvantages. For example, MLR is an easier technique that may be also used by researchers who lack a substantial statistical knowledge and is currently the most used advanced statistical method in paper degradation research. However, this study showed that some variables, which are of well-known relevance to paper degradation but were eliminated during stepwise selection, should be added back as interaction terms. Such additions may negatively balance the multicollinearity mitigation ability of stepwise selection, hence recovering the problem that needed to be solved in the first place and creating a risk of overfitting. Concerning PCR, there is no risk related to multicollinearity, since principal components are orthogonal, and this technique can often reveal underlying mechanisms hidden in the data. Nevertheless, interpretation of principal component analysis frequently represents a difficult task even for researchers with a high level of expertise in multivariate analysis. In general, the application of both methods simultaneously should become an established practice: on the one hand, PCR is a technique with a great potential for revealing new findings in the research field of paper degradation, as long as the principal components are properly interpreted; on the other hand, MLR is still an extremely useful technique, as it can show results that cannot be found using PCR.

There could be further developments in the application of PCR. For instance, in order to interpret the principal components in a better way and to calculate models with substantial information, rotation techniques and cross-validation techniques could be applied [1]. In addition, to increase the prediction power of the models presented in this study, more data should be obtained and, if possible, their measurement precision should be improved. Moreover, if the response variable presents a heterogeneous error distribution, e.g. exponentially distributed rather than normally distributed, it may be useful to calculate a generalised linear model (GLM) [2], although this process is rather complicated and is not commonly used in this area of research. Finally, since the regression coefficients provided by PCR are not guaranteed to be significant, partial least square regression (PLSR) may be a more suitable technique [3]. This method works by projecting both the independent and the response variables to a new space and then constructing a new linear regression model in that space. In this way, while PCR does not transform the response variable, PLSR takes also into account the response variable and may find a model that fits the response better and provides more meaningful results.

References

34. Krzanowski WJ. Cross-validation in principal component analysis. Biometrics 1987;43:575-584.
35. Madsen H, Thyregod P. Introduction to general and generalized linear models. Boca Raton, FL: CRC Press, 2010.
36. Wold S, Sjöström M, Eriksson L. PLS-regression: a basic tool of chemometrics. Chemometr Intell Lab 2001;58(2):109-130.